Acoustooptic Coherent Mode Coupling in Polarization-Maintaining Fiber and Its Application as a Variable-Polarization-Dependent Loss Element

Rong Huang, Fares Alhassen, David Tseng, Ozdal Boyraz, and Henry P. Lee

***Abstract*—In this letter, we investigate coherent acoustooptic coherent mode coupling from the LP_{01} core mode to LP_{1m} cladding mode of a polarization-maintaining fiber (PMF) induced by two acoustic gratings. We show narrowband variable attenuation along either birefringent axis of the PMF by varying the relative phase between the two acoustic gratings. By launching two acoustic gratings at different frequencies, variable attenuation and low crosstalk along either birefringent axis within the acoustooptic coupling bandwidth are demonstrated.**

***Index Terms*—Acoustooptic tunable filter, coherent coupling, piezoelectric transducer (PZT), polarization-dependent loss (PDL).**

I. Introduction

POLARIZATION-MODE dispersion can significantly impair the data-carrying capacity of a telecommunication network in high data rate systems. When polarization-dependent loss (PDL) is also present in the system, further complications result. Therefore, great interest has developed in compensating of PDL. Several variable PDL elements have been investigated, such as two polarization controllers (PCs) [1] and twisted–tilted fiber gratings [2]. Recently, Jung *et al.* [3] reported an all-fiber variable PDL element by inducing acoustooptic mode coupling using a single piezoelectric transducer (PZT) on a polarization-maintaining fiber (PMF). In their experiment, the vibration direction of the acoustic wave is aligned to the fast axis of the PMF in order to achieve a high tuning efficiency. Variable attenuation along this axis is achieved by varying the amplitude of the acoustic wave. In this letter, we demonstrate a variable PDL element on a PMF whereby the attenuation in both slow and fast axes can be achieved independently at the same wavelength using two sets of orthogonally vibrating acoustic waves, each at a different frequency. When used in conjunction with a PDL monitor, the device can be used as an all-fiber on-line PDL compensator.

II. Theory and Experiment

Fiber acoustooptic tunable filter technology provides a unique way to perform wavelength filtering and mode conversion with near-zero insertion loss. In single-mode fiber, a radio-frequency (RF) flexural acoustic wave actuated by a PZT and propagating along a bare fiber can induce mode coupling between core and anti-symmetrical cladding modes when the phase-matching condition is satisfied. Since the cladding mode is eventually absorbed by the fiber jacket, the mode coupling results in a notch-filter-like transmission spectrum where the notch wavelength and the depth of the notch can be tuned by varying the frequency and the amplitude of the acoustic wave, respectively. For polarization related applications, the acoustooptic interaction on PMF is of special interest due to its built-in birefringent properties. A distinguishing feature of PMF is that the presence of strain-induced members inside these fibers not only induces birefringence for the core modes but also for lower order cladding modes [4]. This causes mode coupling to occur only between core and cladding modes having the same polarization. For example, a polarization extinction ratio >15 dB has been shown in PMFs [3]. In addition, the lower order cladding modes are localized in the region between the stress members independent of the orientation of acoustic-induced index perturbation, as illustrated in Fig. 1(a). Since the degeneracy is removed for both core and cladding modes, the resonances for polarizations parallel to fast and slow axes are separated in wavelength: the magnitude of the separation varies from one type of PMF to another.

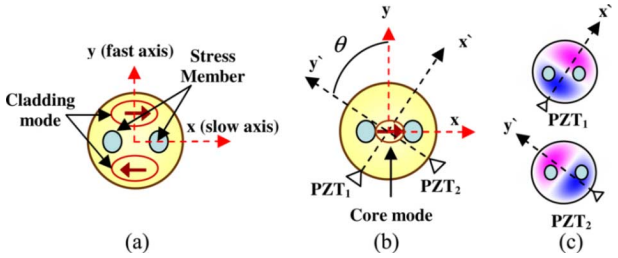

Fig. 1. (a) Localization of lower order cladding mode in regions away from stress member. (b) Vibration directions for a dual-transducer with respect to the birefringence axes of the fiber. (c) Perturbation profile introduced by each PZT.

Fig. 1(b) shows the direction of acoustic vibrations with respect to the birefringence axes of a PMF when an orthogonally vibrating dual-PZT is employed. The slow and fast axes of the PMF are aligned to x and y axes, respectively; PZT_1 and PZT_2 are aligned to x′ and y′ axes, respectively; and θ is the angle between x and x′ (and y′ and y). The index perturbation profile due to the acoustic wave is shown in Fig. 1(c). Consider x-polarized input light. The coupling coefficient between LP_{01} core mode and the anti-symmetrical LP_{1m}-like mode due to PZT_1 has a θ dependence of

Manuscript received January 7, 2007; revised February 8, 2007.

The authors are with the Department of Electrical Engineering and Computer Science, The Henry Samueli School of Engineering, University of California, Irvine, Irvine, CA 92697 USA (e-mail: rongh@uci.edu).

Color versions of one or more of the figures in this letter are available online at http://ieeexplore.ieee.org.

Digital Object Identifier 10.1109/LPT.2007.894339

$$\kappa = \int_{\pi-\theta}^{} \int E_{\mathrm{cl}}(r,\phi)\Delta n(\phi)E_c(r)rdrd\phi$$
$$\propto \int_{-\theta}^{} \sin(\phi)\sin(\phi+\theta)d\phi \propto \cos\theta. \quad (1)$$

This $\cos\theta$ dependence of the effective coupling coefficient has been observed previously and used as a means to align the birefringent axes of a PMF [4]. It also explains why the acoustic vibration has to be aligned close to the fast axis of the PMF in order to achieve a high coupling efficiency. When two acoustic gratings are copropagating, the coupled mode equation for x-polarized core and cladding modes are modified as follows:

$$\frac{d}{dz}E_x^{\mathrm{co}} = -\left(i\kappa_{1,x}^* + i\kappa_{2,x}^*\right)E_x^{\mathrm{cl}}$$
$$\frac{d}{dz}E_x^{\mathrm{cl}} = -\left(i\kappa_{1,x} + i\kappa_{2,x}\right)E_x^{\mathrm{co}} \quad (2)$$

where E_x^{co} and E_x^{cl} are the amplitudes of the x-polarized core and cladding modes, respectively, and $\kappa_{1,x}$ and $\kappa_{2,x}$ are the coupling coefficients induced by acoustic grating 1 and 2, respectively. The effective coupling coefficient, $\kappa_x^e = \kappa_{1,x} + \kappa_{2,x}$, is proportional to $A_1\sin\theta + A_2\cos\theta$, where A_1 and A_2 are complex amplitudes of the acoustic grating 1 and 2, respectively. For weak coupling, $E_x^{\mathrm{cl}} \propto \kappa_x^e E_x^{\mathrm{co}}$. If we set the projected amplitude of each coupling coefficient along the fast axis equal for both gratings, i.e., $|A_2|\cos\theta = |A_1|\sin\theta = A_o$, the out-coupled cladding mode intensity, $I_x^{\mathrm{cl}}(I_x^{\mathrm{cl}} = |E_x^{\mathrm{cl}}|^2)$, which is eventually lost to the fiber jacket takes the form

$$I_x^{\mathrm{cl}} \propto 2A_o^2(1+\cos\alpha)\,|E_x^{\mathrm{co}}|^2 \quad (3)$$

where α is the phase difference between A_1 and A_2.

Equation (3) shows that by varying α we can vary the amount of light coupled to the cladding mode and thus tune the attenuation of x-polarized core mode. Simply put, each of the two orthogonal acoustic waves has a projection along the fast axis of the PMF. When the components along the fast axis are in phase $(\alpha = 0°)$, they add constructively, leading to maximum attenuation of the core mode. If they are out of phase $(\alpha = 180°)$, they cancel out, resulting in zero attenuation of the core mode. An arbitrary value of attenuation between those two bounds can be achieved by varying α. In order to use the dual-PZT as a tunable PDL element on PMF, a simple tuning scheme is used: the projected amplitudes along the fast axis for each acoustic wave are first adjusted to be equal. The attenuation level can then be continuously tuned from this maximum value (set by A_o) all the way down to zero by varying the phase α between the two gratings. The advantage of the dual-PZT approach over its single PZT counterpart is two-fold: 1) alignment of PMF's fast axis to a PZT is no longer required, and 2) a constant power is being applied to the PZT during the entire operation. This helps to achieve better thermal stability for the device.

III. Results and Discussion

Fig. 2 shows the experimental setup of the dual-PZT-based PDL element. A polarized broadband light-emitting diode source and an optical spectrum analyzer (OSA) are used to measure the transmission spectra. The input polarization was

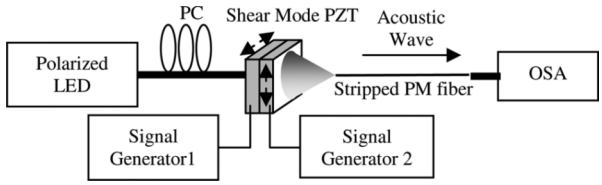

Fig. 2. Experimental setup of the PDL element.

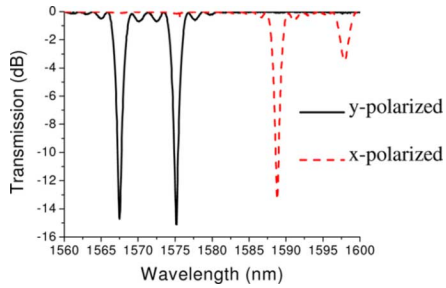

Fig. 3. Transmission spectra for x- and y- polarized core modes light at acoustic frequency of 1.7184 MHz.

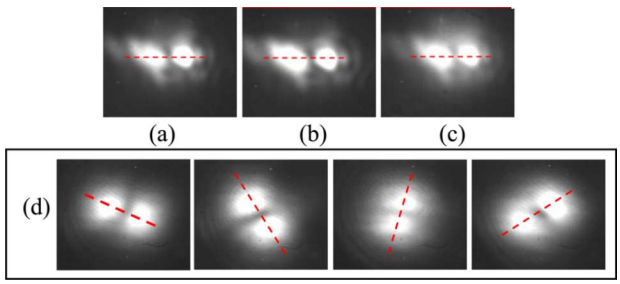

Fig. 4. (a)–(c) Near-field patterns of LP_{11} cladding mode for a PMF when we varied α. (d) Corresponding patterns for a circular symmetric DCF. In both cases, laser light aligned to a fixed birefringent axis is used as the input.

controlled using a PC. The dual-PZT is constructed from a pair of shear mode PZTs as described in [5]. The PMF we used is a 30-cm-long jacket-stripped Fujikura PANDA PMF [4]. Two phase-locked signal generators are used to drive the dual-PZT. Fig. 3 shows the measured transmission spectra for the PMF at a single acoustic frequency when the input light is aligned to either x or y axis. The two groups of polarization-dependent resonances are widely tunable over the entire S-, C-, and L-bands by varying the acoustic frequency. The near-field pattern of coupled LP_{11} cladding mode at different α is imaged using a laser light aligned to one of the birefringent axes, as shown in Fig. 4(a)–(c). Notice that the field patterns are aligned to a fixed direction, independent of vibrating direction. This confirms that the low-order cladding modes are localized in PMFs. In contrast, the LP_{11}-like cladding mode pattern rotates in a circular-symmetric dispersion-compensation fiber (DCF) when α (vibration direction) is varied as shown in Fig. 4(b).

To implement a variable attenuator for x-polarized light, we first align the input light along the x axis. We then turn on only PZT_1 and adjust the voltage so that the attenuation is about 1 dB at the desired resonant wavelength as measured by the OSA. Next, we turn on only PZT_2 and adjust the voltage so that the same attenuation is attained. At these settings, $|A_1|\sin\theta = |A_2|\cos\theta = A_0$. We then adjust the α between the two PZTs. Fig. 5(a) shows the transmission spectra as we vary α in steps

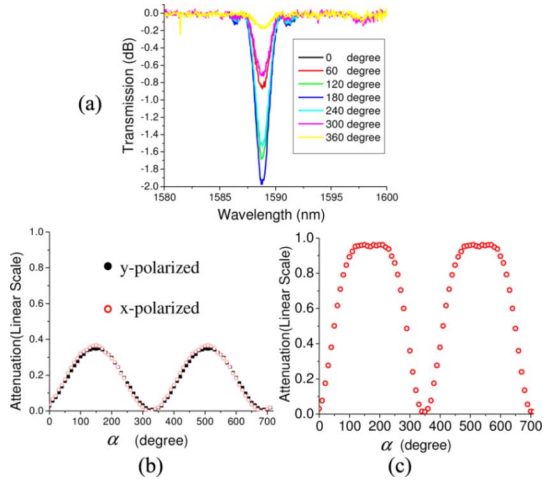

Fig. 5. (a) Transmission spectra versus α for x-polarized core mode light near 1588.55 nm. (b) Attenuation for x- and y-polarized light versus α at λ of 1588.88 and 1575.08 nm, respectively, at acoustic frequency of 1.7184 MHz. (c) Plot of attenuation for x-polarized light versus α at higher attenuation level.

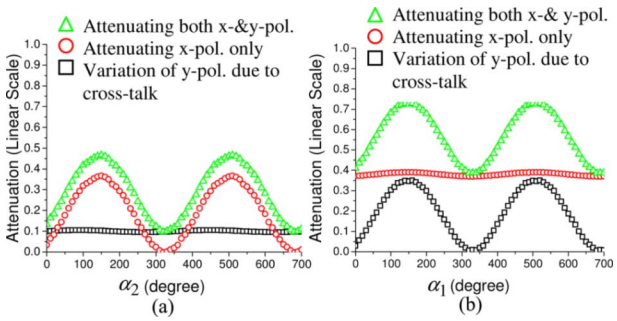

Fig. 6. Crosstalk between attenuation in x- and y-polarized light: (a) tuning attenuation of x-polarized light when attenuation of y-polarized light is set at $\sim$10%; (b) tuning attenuation of y-polarized light when attenuation of x-polarized light is set at $\sim$38%.

of 10° at an acoustic frequency (f_1) of 1.7184 MHz for x-polarized core mode light. The peak attenuation (in linear scale) at 1588.88 nm versus α is plotted in Fig. 5(b) in hollow circle. The results are in excellent agreement with prediction from (3). The phase shift of the maximum attenuation away from the origin $(\alpha = 0)$ is attributed to the propagation delay between the two acoustic waves due to the stacking geometry of the dual-PZT. For y-polarized light, the same procedure is repeated and the results are plotted in solid dots also in Fig. 5(b) at λ of 1575.08 nm. It matches precisely with x-polarized light indicating that the distribution of the field pattern of lower order cladding mode in PMF is identical for both polarizations, thus validating the coupling model for PMF we use here. Next, we repeat the same procedure for x-polarized core mode light but set the maximum attenuation to a higher value. The results are shown in Fig. 5(c) which is in good agreement with prediction from coupled-mode equation (3).

To examine if we can *independently* attenuate both x- and y-polarized core mode light at the same λ, we applied a second set of RF voltages to the dual-PZT at a different frequency f_2 (1.7755 MHz) so that the resonant wavelength for x-polarized coupling coincides with that of the y-polarized coupling at 1575.08 nm. All together, we are applying two pairs of signals to the dual-PZT: $A_1(f_1)$ and $A_2(f_1)$, which attenuate y-polarized core mode light and $A_1(f_2)$ and $A_2(f_2)$, which attenuate x-polarized core mode light, all at a wavelength of 1575.08 nm. The acoustic amplitudes at f_2, namely, $A_1(f_2)$ and $A_2(f_2)$, are adjusted to have the same *projected coupling*. Neglecting crosstalk between PZTs, we expect the total attenuation at the resonant wavelength be an incoherent sum of the attenuation of both x- and y-polarized core modes.

Fig. 6(a) shows the measured maximum attenuation using a polarized broadband light at an arbitrary polarization at λ of 1575.08 nm. We first apply signals at $f_2(A_1(f_2), A_2(f_2))$ to attenuate x-polarized light and vary α_2 while turning off signals at f_1. The attenuation is shown in circles (red) in Fig. 6(a). We then repeat the experiment by turning on signals at $f_1(A_1(f_1), A_2(f_1))$ but setting the attenuation for the y-polarized light to a fixed value ($\sim$10%). The result is shown in the triangles (green) in Fig. 6(a). The difference of the attenuation between triangles (green) and circles (red) is approximately 10% and the crosstalk manifested in the attenuation of y-polarized light due to attenuation of x-polarized light is about -13 dB. Next, we apply signals at $f_1(A_1(f_1), A_2(f_1))$ to attenuate y-polarized light and vary α_1 while leaving signals at f_2 off. The result is shown in black in Fig. 6(b). We then repeat the experiment by turning on signals at $f_2(A_1(f_2), A_2(f_2))$ and setting the attenuation of x-polarized light to a fixed value ($\sim$38%). The result is shown in triangles (green) in Fig. 6(b). The crosstalk of attenuating x-polarized light due to attenuation of y-polarized light is as low as -16 dB. These results show that we can *independently* attenuate both x- and y-polarized core modes light without incurring large crosstalk. However, when we increase the attenuation level in either polarization beyond 5 dB, significant crosstalk occurs due to thermal heating of the PZTs. The problem can be mitigated by using a more efficient PZT/horn design or by adding a thermoelectric cooler to the PZT.

IV. Conclusion

We have investigated coherent acoustooptic mode coupling in PMF and its application as an all-fiber-based PDL element. We show that attenuation in both birefringent axes can be independently controlled with minimum crosstalk when two sets of control signals at two different frequencies are applied to the dual-PZT.

References

[1] L.-S. Yan, Q. Yu, and A. E. Willner, "Demonstration of in-line monitoring and compensation of polarization-dependent loss for multiple channels," *IEEE Photon. Technol. Lett.*, vol. 14, no. 6, pp. 864–866, Jun. 2002.

[2] P. Reys, M. Fishteyn, S. Wielandy, and P. Westbrook, "Tunable PDL of twisted-tilted fiber gratings," *IEEE Photon. Technol. Lett.*, vol. 15, no. 6, pp. 828–830, Jun. 2003.

[3] H. G. Jung, S. H. Lee, H. C. Ji, B. Y. Kim, and S.-Y. Shin, "Tunable polarization-dependent loss element based on acoustooptic mode coupling in a polarization-maintaining fiber," *IEEE Photon. Technol. Lett.*, vol. 16, no. 6, pp. 1510–1512, Jun. 2004.

[4] C.-H. Lin, Q. Li, and H. P. Lee, "Periodic microbending-induced core-to-cladding mode coupling in polarization-maintaining fibers," *Opt. Lett.*, vol. 28, no. 12, pp. 998–1000, 2003.

[5] P. Z. Dashti, Q. Li, C.-H. Lin, and H. P. Lee, "Coherent acousto-optic mode coupling in dispersion compensating fiber by two acoustic gratings with orthogonal vibration directions," *Opt. Lett.*, vol. 28, pp. 1403–1405, 2003.